Application of Nickel (II) Complex of Dithiocarbamate-Modified Starch for Anionic Dyes Removal from Aqueous Solutions

Rumei Cheng,[1] Bo Xiang,[2] Yijiu Li[2]

[1]*Institute of Advanced Materials for Nano-Bio Applications, School of Ophthalmology and Optometry, Wenzhou Medical College, China*
[2]*Department of Chemistry, Tongji University, China*

Received 19 March 2011; accepted 2 May 2011
DOI 10.1002/app.34836
Published online 25 August 2011 in Wiley Online Library (wileyonlinelibrary.com).

ABSTRACT: The work presents the synthesis of nickel (II) complex of dithiocarbamate-modified starch (DTCSNi). It is characterized by elemental analysis, infrared spectrum, and thermogravimetry methods. A batch system was applied to study the adsorption of DTCSNi for four anionic dyes removals. The adsorption with respect to the pH was investigated. It is found that the capacity of DTCSNi for each dye is pH dependent, and the adsorption is governed by coordination. At the suitable pH 4, two kinetic models, that is, pseudo-first- and pseudo-second-order, were tested to investigate the adsorption process. The kinetic parameters of the models were calculated and discussed. The results suggest that the best fit model is the pseudo-second-order equation. The Langmuir–Freundlich model agrees very well with experimental data and the maximum adsorption capacity sequence is AO7 > AG25 > AR18 > AO10. The Fourier transform infrared spectra and thermogravimetric analysis verified the chelating molecular mechanism. © 2011 Wiley Periodicals, Inc. J Appl Polym Sci 123: 2439–2444, 2012

Key words: modified starch; nickel complex; anionic dyes; adsorption; infrared spectra

INTRODUCTION

Wastewaters discharged by textile industries are known to contain large amounts of dyes. Dyes are hazardous pollutants, causing environment and health problems to mankind and aquatic organism.[1,2] Because dyes are toxic chemicals, it is necessary to remove the dyes from industrial effluents before they are discharged into the environment. There are diverse treatment methods those have been applied for dyes removal, such as activated sludge,[3] chemical oxidation,[4] photodegradation processes,[5] and adsorption procedures.[6,7] Adsorption processes have long been studied and recognized as one of the most important techniques.[8] Proper selection of adsorbent using in the adsorption procedure will produce high-quality treated effluents. So far, diverse adsorbents are tested for dyes removal. Most of them are inorganic adsorbent (activated carbon,[9] zeolites,[10] etc.) and organic adsorbents (chitosan,[11] modified starch,[12] etc.).

Many organic adsorbents have been applying for treatment of heavy metal polluted water, producing metal complexes. Such complexes are always regarding as waste residues. Recently, people found that some metal complexes are practical adsorbents for separation and removal of dyes.[13] In our previous work,[14] the copper complex of dithiocarbamate-modified starch (DTCS) was used to adsorb acid dyes. The copper complex of DTCS (DTCSCu) has a dinuclear structure. And the equilibrium studies on dyes adsorption on DTCSCu showed one dye molecule chelating to two close copper ions. However, the kinetics study is neglected. Also, the fixation abilities of DTCS for various transition metals are different, particularly between copper and nickel.[15] The structure of nickel complex of DTCS (DTCSNi) is not clear. The behaviors of individual complexes are strongly affected by their structures. To investigate the structure difference between nickel complex and copper complex of DTCS (DTCSNi and DTCSCu), we use the dyes as sensors to probe the surface structure of DTCSNi. It should be interesting to find out whether the DTCSNi has a similar adsorption behavior as DTCSCu. So far, the knowledge of applying heavy metal complexes for fixation dyes is limited. In the article, the adsorption kinetics and equilibrium were carefully studied. The structure of DTCSNi and its adsorption performance have been clarified. As a result, the DTCSNi showed superior adsorption properties for anionic dyes removal, being a promising adsorbent.

Correspondence to: R. Cheng (rumeicheng@yahoo.com).
Contract grant sponsor: Science Foundation of Wenzhou Medical College; contract grant number: KYQD110104

TABLE I
List of Anionic Dyes Investigated in this Study

Generic name	Abbreviation	Fw	Structure	λ_{max} (nm)
Acid orange 7	AO7	350.3	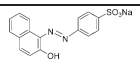	485
Acid orange 10	AO10	452.4	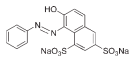	475
Acid red 18	AR18	604.5	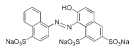	506
Acid green 25	AG25	622.6	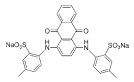	642

EXPERIMENTAL

Materials

Commercial corn starch, of food-grade quality, was used in this research. Nickel (II) chloride ($NiCl_2{\cdot}6H2O$) and other routine reagents were of analytical grade. Four commercially available dyes, acid orange 7 (AO7), acid orange 10 (AO10), acid red 18 (AR18), and acid green 25 (AG25), were purchased from Sigma and used as received. They have been widely studied as typical contaminants in wastewater. The molar mass and charges often affect the sorption behavior. The four dyes have sulfonate groups with negative charges but difference in molar mass and charges. Also, their structures are slightly different. The chemical structures and characteristics of the four dyes are shown in Table I.

Techniques

The elemental analyses were performed with a Perkin-Elmer 240C elemental analyzer. Fourier transform infrared spectra (FTIR) were recorded on a Perkin Elmer Spectrum One spectrometer with KBr pellets in the 4000–450 cm^{-1} region. Ultraviolet-visible (UV-vis) spectra were measured with a Perkin-Elmer Lambda 35 spectrometer. Thermogravimetric analyses were performed with STA 409 PC/4/H Luxx at a heating rate of 10°C/min under a N_2 atmosphere.

Preparation of DTCSNi

The DTCS was first synthesized as reported previously,[16] and the process is shown in Figure 1. Then 10.0 g of dried DTCS was added to a 500 mL solution containing 3.0 g of $NiCl_2{\cdot}6H_2O$ at pH 5.0. The mixture was stirred for 12 h at 25°C, and the precipitate was separated from the solution. The Ni^{2+}-saturated polymer was washed five times with deionized water. The acquired DTCSNi was kept in a vacuum oven for 1 day and stored in a desiccator. Found: C 46.53%, H 8.41%, N 2.97%, S 4.57%, Ni 1.58%.

Concentration measurement calibration

To determine the dye concentration in the solution, a calibration curve was first obtained using a UV-vis spectrophotometer. The maximum absorbance of each dye was confirmed by scanning the dye aqueous solution over the spectral range of 200–800 nm. A series of dye solutions with various concentrations was used for the measurement of a calibration curve. A linear relationship between the absorbance (at the wavelength of maximum absorbance, λmax) and the dye concentration was obtained.

Sorption experiments

Adsorption studies were performed using a batch technique. The effect of pH was observed by studying the adsorption of each dye over a pH range of 3–9. For these experiments, a series of 100 mL conical flasks were used. Each flask was filled with 50 mL of a dye solution for a concentration of 300 mg L^{-1} at different pHs. The flasks were shaken for 12 h in a shaking thermostatic bath to reach equilibrium. After filtration, the concentrations of each dye in the aqueous solutions were measured.

For the equilibrium adsorption studies, a fixed mass of DTCSNi (0.1500 g) was weighed into the flasks with a 50 mL solution containing a known amount of the respective dye (varying from 300 to 1200 mg L^{-1}). The pH of the solution was adjusted to 4.0 and kept constant. The flasks were agitated for 24 h in a shaking thermostatic bath. The temperature was maintained at 25°C. After filtration, the concentration of each dye solution was determined. The results were then used to calculate the loading of each dye onto DTCSNi, using eq. (1):

$$q_e m = (c_0 - c_e)V \tag{1}$$

where q_e is the dye concentration in the solid phase (adsorbent) at equilibrium (mmol g^{-1}), m is the mass

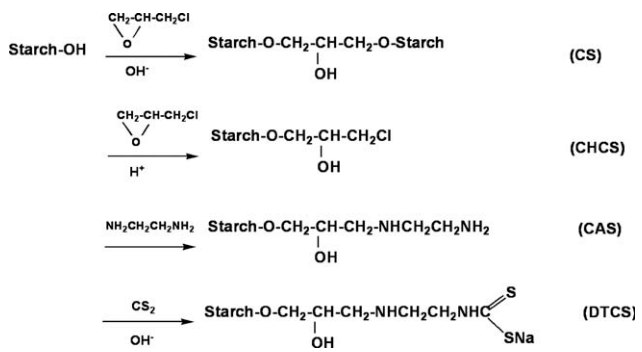

Figure 1 Synthesis of DTCS.

of DTCSNi used (g), c_0 is the initial dye concentration in the liquid phase (mmol L^{-1}), c_e is the dye concentration in the liquid phase at equilibrium (mmol L^{-1}), and V is the total volume of the solution used (L). The models of the isotherms were fitted to equilibrium data using a nonlinear method, with the nonlinear fitting facilities of the Microcal Origin 7.0 software.

Adsorption isotherms

The well-known Langmuir isotherm was originally proposed to describe the adsorption of gas molecules onto metal surfaces.[17] The model assumes uniform energy of the adsorption onto the surface and no migration of the adsorbate in the plane of the surface. The Langmuir adsorption isotherm has been applied successfully to many other real situations of monolayer adsorption.[18] It is expressed as

$$q_e = \frac{abc_e}{1 + bc_e} \tag{2}$$

where q_e is the adsorbed amount of the dye at equilibrium (mmol g^{-1}), c_e is the adsorbate concentration at equilibrium in aqueous solution (mmol L^{-1}). The Langmuir isotherm parameters are a and b. The capacity of the adsorbent can be evaluated by a, and the parameter b includes various physical constants.[19] Another isotherm is represented using eq. (3) known as the Freundlich equation which describes heterogeneous systems,[20] i.e., surfaces with nonenergetically equivalent sites. It is an empirical equation and can be written as follows:

$$q_e = K_f c_e^{1/n} \tag{3}$$

where K_f is the Freundlich constant being indicative of the extent of sorption, and $1/n$ is the heterogeneity factor being an indicator of sorption effectiveness.

Another useful equation is the Langmuir-Freundlich isotherm,[21] which includes three parameters. This isotherm is based on the generalized Langmuir and generalized exponential isotherms[22] and is the most promising extension of the Langmuir and Freundlich isotherms. The Langmuir-Freundlich isotherm is expressed as

$$q_e = \frac{q_m (K_{lf} c_e)^v}{1 + (K_{lf} c_e)^v} \tag{4}$$

where q_m is the maximum adsorption (mmol g^{-1}), K_{lf} is the Langmuir-Freundlich constant (L $mmol^{-1})^{1/v}$, and v is the Langmuir-Freundlich heterogeneity constant. The Langmuir-Freundlich isotherm is essentially the Freundlich isotherm approaching a maximum at high concentrations.

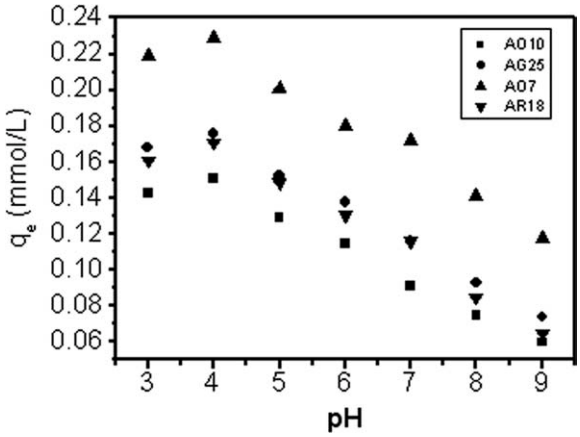

Figure 2 Effect of pH value on adsorption of anionic dyes onto DTCSNi.

RESULTS AND DISCUSSION

Influence of pH

In dye adsorption process, the pH value of aqueous solution is an important parameter; it has significantly influence on the adsorption capacity. The influence of solution pH was observed in a pH range of 3–9.The dyes molecules are stable in the pH range of 3–9. From Figure 2, we can see that DTCSNi for each dye was pH dependent, and adsorption capacity decreased with the increase of pH value. The investigation shows that ZnO[23] and activated carbon modified with Y^{3+} ions[24] also have pH-dependent trend, it suggests that the anionic dyes interact with metal centers and lead the adsorption process. In a dye solution, the free hydroxyl ions and large numbers of water molecules approached the Ni^{2+} center of DTCSNi because of its positive charge and coordination properties. At the same time, the dye molecules, which contain sulfonate groups with negative charges, changed places with the water molecules or hydroxyl ions to chelate the Ni^{2+} ions, resulting in their stronger adsorption. With the increase of pH value, the adsorption capacity for each dye decreases because more free hydroxyl ions formed and interacted strongly with the nickel ions, preventing the dyes from chelating the Ni^{2+} on the polymer surface. So the adsorption capacity decreased when the solution pH increased.

Effect of kinetics model and contact time

To evaluate the effectiveness of the adsorbate and sorption mechanism, studies on kinetics of adsorption processes are necessary. A simple kinetic analysis of adsorption is the pseudo-first-order equation[25] in the form

$$q_t = q_e(1 - e^{=k_1 t}) \tag{5}$$

A pseudo-second-order equation[26] was also tested on the experimental data. The kinetic rate equation is

TABLE II
Parameters of Kinetic Models for Dyes Adsorption on DTCSNi

	Pseudo-first-order			Pseudo-second-order			
Dye	k_1 (min $^{-1}$	q_e (mmol g^{-1})	R^2	k_2 (g mmol^{-1} min^{-1})	q_e (mmol g^{-1})	h (mmol g^{-1} min^{-1})	R^2
AO7	0.059	0.240	0.902	0.338	0.257	0.022	0.981
AO10	0.072	0.148	0.882	0.649	0.158	0.016	0.975
AG25	0.097	0.178	0.889	0.740	0.188	0.026	0.979
AR18	0.059	0.169	0.915	0.524	0.179	0.017	0.980

$$q_t = \frac{k_2 q_e^2 t}{1 + k_2 q_e t} \quad (6)$$

Where q_t is the amount of dye on the sorbent (mmol g^{-1}) at any time t (min), q_e is the amount of dye absorbed at equilibrium (mmol g^{-1}), k_1 is the rate constant of pseudo-first-order adsorption (min^{-1}) and k_2 is the rate constant of pseudo-second-order adsorption (g mmol^{-1} min^{-1}). In most studied adsorption systems, the pseudo-first-order equation is generally applicable over the first 20–30 min of the sorption process and does not fit well over the entire adsorption period. In this experiment, there is a high match between pseudo-second-order equation and the experimental results for the four dyes, as shown in Table II, the pseudo-second-order predicted all dyes are the most agreeing values with the experimental data (Fig. 3 and Table II). According to the kinetic modeling results, the pseudo-second-order model shows the best fit to the experimental data related to the biosorption of used dyes onto DTCSNi. The kinetics of dyes adsorption onto DTCSNi obtained by batch contact time studies was showed in Figure 3. The plot represents the amounts of dyes adsorbed onto DTCSNi versus time, for an initial dye concentration of 1.0 mmol L^{-1}.The adsorption process of DTCSNi is slow, and adsorption capacity of DTCSNi is steady increase and achieves equilibrium after 300 min. The sorption rate is not only related with molecular size of dyes but also with molecular structure, this can be proved by the initial adsorption rates of AO7 and AG25, which were faster than those of AR18 and AO10. The reason is that sulfonate groups of AO7 and AG25 lie in benzene ring and sulfonate groups of AR18 and AO10 lie in naphthalene ring. The adsorption behavior of DTCSNi is different with DTCSCu, this is that the coordination behaviors of copper and nickel ion are different on DTCS.

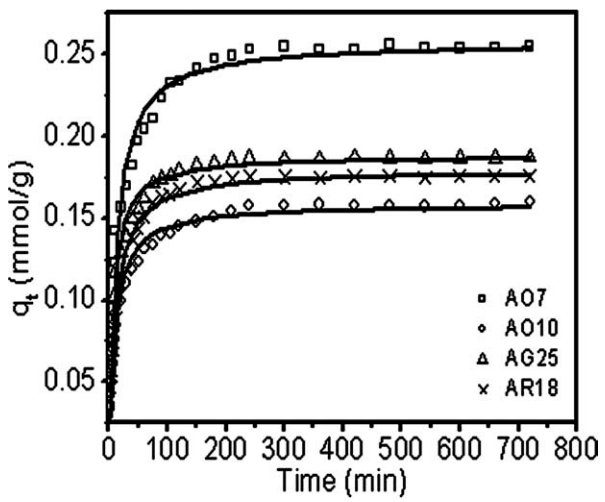

Figure 3 Kinetics of dyes adsorption onto DTCSNi for an initial concentration of 1.0 mmol L^{-1}. Lines represent modeled results using the pseudo-second-order equation.

Adsorption equilibrium and molecular mechanism

Adsorption isotherms are important in optimizing the use of adsorbents, it describe how adsorbates interact with adsorbents. The experiment results are showed in Figure 4 and Table III. The Langmuir-Freundlich isotherm shows the coefficient (R^2) of adsorption is satisfied for each dye and clearly provides satisfactory fits for the four dyes. The adsorption capacity of DTCSNi for four dyes follows the sequence AO7 > AG25 > AR18 > AO10. We can see that the capacities are not related to the charges of dyes but molecular size and structure. AO7 is the smallest molecular of four dyes and has the highest capacity in four dyes. Capacity of the other molecular is related to molecular structure. The anionic dyes with sulfonate groups on benzene are better adsorbed than those with sulfonate groups on

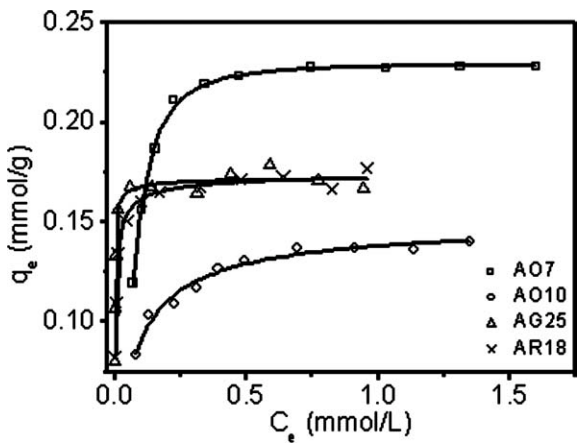

Figure 4 Adsorption isotherms fitted to Langmuir-Freundlich equation (the real lines).

TABLE III
Parameters of Langmuir-Freundlich Isotherm for Dyes Adsorption onto DTCSNi

Dye	q_m (mmol g^{-1})	K_{lf} ($L^{1/v}$ $mmol^{-1/v}$)	v	R^2	Molar ratio n(dye) : n(Ni)
AO7	0.229	14.86	0.870	0.998	1.19
AO10	0.151	16.39	0.884	0.974	0.78
AG25	0.176	3988.55	0.583	0.983	0.92
AR18	0.171	685.88	0.559	0.990	0.90

naphthalene. Although the molecular size of AO10 is close to that of AO7, the capacity for AO10 is lower, which is attributed to the sulfonate groups located on the naphthalene ring. Study indicated that the capacity of activated bleaching earth for AO10 was much lower than those of anionic dyes containing sulfonate groups on benzene rings.[27] The experiment result showed that AG25 (with sulfonate groups on benzene rings) has much higher capacity than AR18 (with sulfonate groups on naphthalene rings). From the dyes molecular structure, we can see that the sulfonate groups of AR18 and AO10 are all located on the naphthalene ring. However, the AR18 produces a greater conjugated effect than that observed for AO10 because more naphthalene rings exist in the AR18. The stronger conjugated effect stabilizes the sulfonate anion and enhances its acidity. Then AR18 is relatively hard to combine with free H^+ ions in aqueous solution and has a much stronger capacity to bond metal ions than does AO10.

From the experiment result, we can see that capacity sequence for individual dyes is very similar as DTCSCu belonging to coordination adsorption.[14] But molar n(dye) : n(Ni) ratio is different from that of n(dye) : n(Cu). The metal complex of DTCSCu has dinuclear copper structure and molar n(dye) : n(Cu) ratio is approximately 1 : 2, except for AO7 (with a molar ratio of 1 : 1). But from Table III, we can see that molar n(dye) : n(Ni) ratio is near 1 : 1, so it can be speculated that the metal complex of DTCSNi has mononuclear structure, forming the structure of one dye molecular bonding to one nickel ion.

The coordination mode of DTCS with nickel ion can be speculated that it is assign to Figure 5(a,c). Nickel ion has d^8 electron configuration and EPR cannot clearly observe coordination condition of nickel ion. To prove the dyes interacting with DTCSNi, the FTIR spectroscopic method was used. The different FTIR spectra of DTCSNi and the dye loaded DTCSNi are shown in Figure 6. The peaks for dithiocarbamate of DTCSNi appear at 1638 and 1510 cm^{-1}.[28,29] The νC-N (-N-CS_2) vibration peak appears at 1456 cm^{-1}.The peaks at 1409, 1391, and 1203 cm^{-1} are assigned to the coupling of the δO-H and δC-H vibrations. Because various hydrogen bonds is formed in adsorption process and coupling vibration of νC-O and νC-O-C split into multiple peaks. The characteristic peaks of the aromatic rings can be found at 1506, 1428, 1326, and 1269 cm^{-1} after the adsorption of the dyes. However, metal ion chelated to sulfonate groups and caused νSO_2 vibration peaks to broaden obviously.[30] These data show that DTCSNi effectively adsorbs the dyes and sulfonates interact with nickel ions.

Thermal analysis is used for research the stability of DTCSNi before and after adsorption of dyes. From Figure 7, we can see that the DTCSNi-dye shows a lower decomposition rate than that of DTCSNi, indicating formation of a more stable complex. It is to say that thermal stability of DTCSNi enhanced after the dyes chelating to nickel ion. From DSC curves (Fig. 8), we can observe that the curve of DTCSNi has five peaks. The endothermic peak at 80°C corresponds to the loss of bound water. The second weak endothermic peak appears at 250°C in the decomposition of DTCSNi. The reason of endothermic peak for DTCSNi is probably due to the decomposition of dithiocarbamate and hydroxyl. At the same time, the rearrangement of molecules leads to the appearance of another weak endothermic peak. The difference of thermal effect between

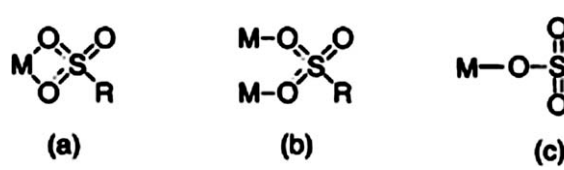

Figure 5 Coordination mode between metal ion and dye molecular.

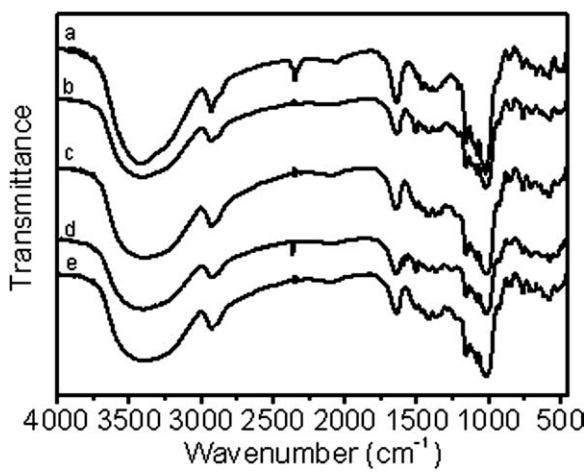

Figure 6 FTIR spectra of DTCSNi before and after adsorption of dyes: (a) DTCSNi; (b) AO7 on DTCSNi; (c) AO10 on DTCSNi; (d) AG25 on DTCSNi; (e) AR18 on DTCSNi.

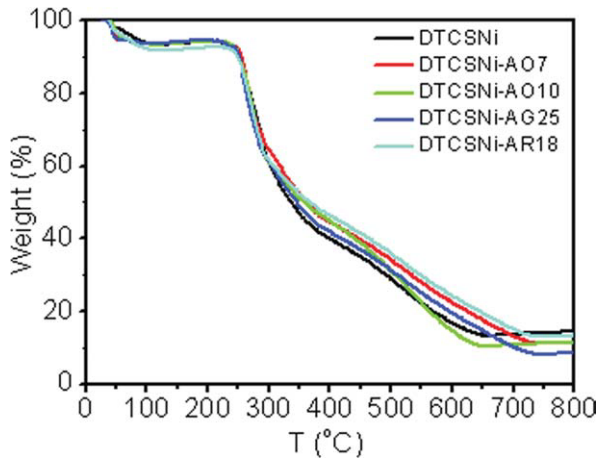

Figure 7 TGA curves of DTCSNi and dye loaded DTCSNi.

DTCSNi and DTCSCu may be related to the structure of the metal complex. After the DTCSNi adsorbed the dyes, this peak shifts to the range of 256–270°C, because of the dyes covering the surface of DTCSNi, affecting its thermal stability. When temperature is over 350°C, the decomposition and carbonization process of polymer and dyes happen.[31,32]

CONCLUSIONS

In this article, we investigated the interaction of the metal complex (DTCSNi) with anionic dyes (AO7, AO10, AG25, and AR18). The research result showed that the capacity of DTCSNi is pH dependent, furthermore, adsorption capacity related to molecular size and structure. The sequence of adsorption capacity is followed the AO7 > AG25 > AR18 > AO10, and adsorption isotherm of four dyes all best fitted to Langmuir-Freundlich isotherm. For four dyes, the molar n(Ni) : n(dye) ratio was near 1 : 1,suggesting that coordination of one nickel with one dye. The dyes molecular bound to nickel ion by chelation. The thermogravimetric analyses showed that decomposition rates of metal complex of DTCSNi bounding dyes are slower than that of DTCSNi, suggesting forming more stable complex of DTCSNi-dye. Such understanding provides new insights as how to optimize the use of transition metal complex of modified starch.

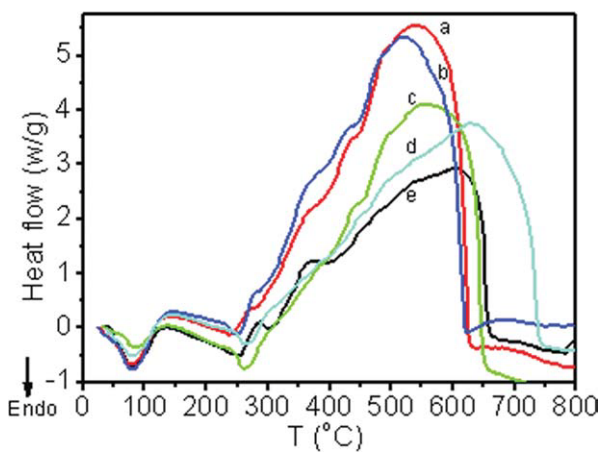

Figure 8 DSC curves of DTCSNi and dye loaded DTCSNi: (a) AO7 bound DTCSNi; (b) AG25 bound DTCSNi; (c) AO10 bound DTCSNi; (d) AR18 bound DTCSNi; (e) DTCSNi.

References

1. Pearce, C. I.; Lloyd, J. R.; Guthrie, J. T. Dyes Pigm 2003, 58, 179.
2. Crini, G. Bioresour Technol 2006, 97, 1061.
3. Bahte, S.; Schwarzenbeck, N.; Hausner, M. Bioresour Technol 2009, 100, 2902.
4. Muthukumar, M.; Sargunamani, D.; Selvakumar, N. Dyes Pigm 2005, 65, 151.
5. Zhao, X.; Qu, J. H.; Liu, H. J.; Hu, C. Environ Sci Technol 2007, 41, 6802.
6. Blackburn, R. S. Environ Sci Technol 2004, 38, 4905.
7. Kron, D. A.; Holland, B. T.; Wipson, R.; Maleke, C.; Stein, A. Langmuir 1999, 15, 8300.
8. Rio, S.; Faur-Brasquetc, C.; Le Coq, L.; Le Cloirec, P. Environ Sci Technol 2005, 39, 4249.
9. Aber, S.; Daneshvar, N.; Soroureddin, S. M.; Chabok, A.; Asadpour-Zeynali, K. Desalination 2007, 211, 87.
10. Qiu, M. Q.; Qian, C.; Xu, J.; Wu, J. M.; Wang, G. X. Desalination 2009, 243, 286.
11. Cheung, W. H.; Szeto, Y. S.; McKay, G. Bioresource Technol 2009, 100, 1143.
12. Cheng, R.; Ou, S.; Li, M.; Li, Y.; Xiang, B. J Hazard Mater 2009, 172, 1665.
13. Jang, M.; Min, S. H.; Park, J. K.; Tlachac, E. J. Environ Sci Technol 2007, 41, 3322.
14. Cheng, R.; Ou, S.; Xiang, B.; Li, Y.; Liao, Q. Langmuir 2010, 26, 752.
15. Liao, Q.; Li, Y.; Xiang, B. Fine Chem 2008, 25, 281.
16. Xiang, B.; Li, Y. J.; Ni, Y. M. J Appl Polym Sci 2004, 92, 3881.
17. Langmuir, I. J Am Chem Soc 1918, 40, 1361.
18. Blackburn, R. S.; Harvery, A.; Kettle, L. L.; Payne, J. D.; Russell, S. J. Langmuir 2006, 22, 5636.
19. Giles, C. H.; Smith, D.; Huitson, A. J Colloid Interface Sci 1974, 47, 755.
20. Freundlich, H. M. F. Z Phys Chem 1906, 57, 385.
21. Marczewski, A. W.; Derylo-Marczewska, A.; Jaroniec, M. J Chem Soc Faraday Trans 1988, 84, 2951.
22. Lazaridis, N. K.; Kyzas, G. Z.; Vassiliou, A. A.; Bikiaris, D. N. Langmuir 2007, 23, 7634.
23. Bauer, C.; Jacques, P.; Kalt, A. Chem Phys Lett 1999, 307, 397.
24. Tamai, H.; Yoshida, T.; Sasaki, M.; Yasuda, H. Carbon 1999, 37, 983.
25. Ania, C. O.; Béguin, F. Water Res 2007, 41, 3372.
26. Hu, J.; Song, Z.; Chen, L.; Yang, H.; Li, J.; Richard, R. J Chem Eng Data 2010, 55, 3742.
27. Tsai, W. T.; Chang, C. Y.; Ing, C. H.; Chang, C. F. J Colloid Interface Sci 2004, 275, 72.
28. Nakamoto, K.; Fujita, J.; Condrate, R. A.; Morimoto, Y. J Chem Phys 1963, 39, 423.
29. Kaul, B. B.; Pandeya, K. B. J Inorg Nucl Chem 1978, 40, 229.
30. Zhao, Y.; Sun, B.; Xu, Y.; Wang, D.; Weng, S.; Wu, J.; Xu, D.; Xu, G. J Mol Struct 2001, 560, 115.
31. Liu, X.; Yu, L.; Liu, H.; Chen, L.; Li, L. Polym Degrad Stab 2008, 93, 260.
32. Vasconcelos, H. L.; Guibal, E.; Laus, R.; Vitali, L.; Favere, V. T. Mater Sci Eng C 2009, 29, 613.